On the distillation and purification of phase-diffused squeezed states

B Hage[1], A Franzen[1], J DiGuglielmo[1], P Marek[2], J Fiurášek[3] and R Schnabel[1]

[1] Max-Planck-Institut für Gravitationsphysik (Albert-Einstein-Institut) and Leibniz Universität Hannover, Callinstr. 38, 30167 Hannover, Germany
[2] School of Mathematics and Physics, The Queens University, Belfast BT7 1NN, United Kingdom
[3] Department of Optics, Palacký University, 17. listopadu 50, 77200 Olomouc, Czech Republic

E-mail: boris.hage@aei.mpg.de

Abstract. Recently it was discovered that non-Gaussian decoherence processes, such as phase-diffusion, can be counteracted by purification and distillation protocols that are solely built on Gaussian operations. Here we make use of this experimentally highly accessible regime, and provide a detailed experimental and theoretical analysis of several strategies for purification/distillation protocols on phase-diffused squeezed states. Our results provide valuable information for the optimization of such protocols with respect to the choice of the trigger quadrature, the trigger threshold value and the probability of generating a distilled state.

PACS numbers: 03.67.-a, 42.50.-p, 03.65.Ud

Submitted to: *New J. Phys.*

1. Introduction

Continuous variable quantum information processing [1] represents an appealing alternative to the traditional qubit based approaches. Continuous quantum variables encoded in quadrature components of light modes [2, 3, 4, 5, 6] or collective atomic spin [7, 8, 9] offer several distinct advantages. Many important quantum information processing primitives could be implemented deterministically with only linear optics, optical parametric amplifiers ("squeezers") and balanced homodyne detection. This includes for example preparation of entangled two-mode squeezed states [2, 10, 11, 12, 13], quantum teleportation [5, 6, 14], dense coding [15], entanglement swapping [16] and quantum cloning [17]. Quantum states of light beams could be deterministically stored in an atomic quantum memory [8] and teleportation of quantum state of a light mode onto the atomic ensemble has been demonstrated [9].

In all these developments, Gaussian states and Gaussian operations play a prominent role. Recall that Gaussian states are states with Gaussian Wigner function and Gaussian operations are those quantum transformations which preserve the Gaussian shape of the Wigner function. Passive linear optics, squeezers and homodyne detection are all examples of Gaussian operations and they allow to prepare arbitrary Gaussian states from coherent states. However, it has been realized that Gaussian operations are insufficient for entanglement distillation of Gaussian states [18, 19, 20]. This is a significant limitation, because entanglement distillation [21, 22] is critical for suppression of noise and losses which inevitably arise during the distribution of entanglement between distant parties. The entanglement purification/distillation protocol extracts a highly entangled pure state from many copies of mixed weakly entangled states using only local operations and classical communication between the parties sharing the states. It is anticipated that any long-distance quantum communication network will have to involve entanglement distillation in some form. A similar no-go theorem has been proved also for the concentration of squeezing [23]. Namely, given an arbitrary N-mode Gaussian state, it is not possible to increase its squeezing strength by passive Gaussian operations. Here, the squeezing strength is quantified by the lowest eigenvalue of the covariance matrix of the state, and passive Gaussian operations are those building on linear optics, homodyning and feedforward. This implies that it is impossible to extract in this way from N copies of a single-mode squeezed Gaussian state a state with higher squeezing.

Continuous-variable entanglement distillation thus requires to go beyond the realm of Gaussian states and operations in at least a single step [24, 25, 26]. A complete protocol for entanglement distillation of Gaussian states has been suggested by Browne, Eisert *et al.* [26, 27]. This protocol consists of two steps. First, the state is de-Gaussified e.g. by conditional subtraction of a single photon [25, 28, 29, 30, 31]. Second, the de-Gaussified states are Gaussified using interference on beam splitters, Gaussian measurements and conditioning. If, however, the dominant noise itself is such that it de-Gaussifies the state, then no further de-Gaussification is necessary and the squeezed or entangled states can be distilled and purified solely by means of passive linear optics, homodyne detection and conditioning [32, 33, 34]. Purification of squeezed states has been demonstrated in this regime in [35]. However, the purification was accompanied with a degraded degree of squeezing. Recently, we have proposed and experimentally demonstrated a protocol for purification *and* distillation of squeezed states suffering from phase fluctuations [33]. These fluctuations, which are an important source of noise in optical communication links, can be suppressed by interference of two copies of the non-Gaussian phase-diffused squeezed state on a balanced beam splitter, followed by homodyne detection on one of the outputs and acceptance or rejection of the resulting state depending on the measurement outcome. Our procedure works for both single-mode and two-mode squeezed states and the latter could be distilled by means of local operations and measurements and classical communication. The purification/distillation procedure could be applied iteratively and could serve as a gaussification part of the

universal CV entanglement distillation protocol based on a sequence of de-Gaussification and Gaussification steps.

In this paper we report on a detailed theoretical and experimental analysis of several strategies for purification/distillation of phase-diffused single-mode squeezed states. Our results provide a detailed insight into the features and properties of the purification/distillation protocol and represent a significant step towards the experimental demonstration of continuous-variable entanglement distillation. Compared to our previous works [32, 33], we do not assume only conditioning on measurements of the initially squeezed amplitude quadrature x_1 but allow for detection of arbitrary quadrature component. We find that the purification/distillation protocol exhibits a far greater richness than expected. Surprisingly enough if, after the interference of the two noisy copies of the state on a beam splitter, we measure the originally anti-squeezed phase quadrature p_1 of the first output beam and condition on $|p_1| < Q$ then this allows an enhancement of the squeezing of the amplitude quadrature x_2 of the second output beam. This is somewhat unexpected since one could naively argue that conditioning on small p_1 should enhance the fluctuations of x_2, see Sec. 2.3. We term this technique conjugate purification (CP). In certain regimes this method is even optimal and for a given amount of distilled squeezing yields higher purification/distillation rates than squeezed quadrature-conditioning. Conditioning on the anti-squeezed quadrature most clearly reveals the quantum nature of our purification/distillation protocol.

The paper is organized as follows. In Section 2 we present our purification/distillation protocol for phase-diffused squeezed states. This section includes its experimental demonstration as well as its theoretical description, and also a comparison of experimental results and theoretical predictions. In Section 3 we investigate quantum channel probing as a classical enhancement of our purification/distillation protocol. Finally, Section 4 contains a brief summary and conclusions.

2. The purification/distillation protocol

The scheme for purification and distillation of phase-diffused single-mode squeezed states is shown in Fig. 1. It is a variant of the scheme originally proposed by Browne *et al.* for Gaussification of continuous-variable entangled states [26]. Two copies of a single-mode squeezed state generated in optical parametric amplifiers (OPA) I and II independently pass through a noisy quantum channel which imposes independent and random phase fluctuations upon each state. These fluctuations reduce the quadrature squeezing and the purity of the state and make it non-Gaussian [33]. For the sake of specificity, we assume that the phase fluctuations exhibit Gaussian distribution with zero mean and variance σ^2,

$$\Phi(\phi) = \frac{1}{\sqrt{2\pi\sigma^2}} \exp\left(-\frac{\phi^2}{2\sigma^2}\right). \tag{1}$$

Note, however, that the exact form of the phase distribution $\Phi(\phi)$ is not essential and our findings presented below qualitatively hold independently of the exact form

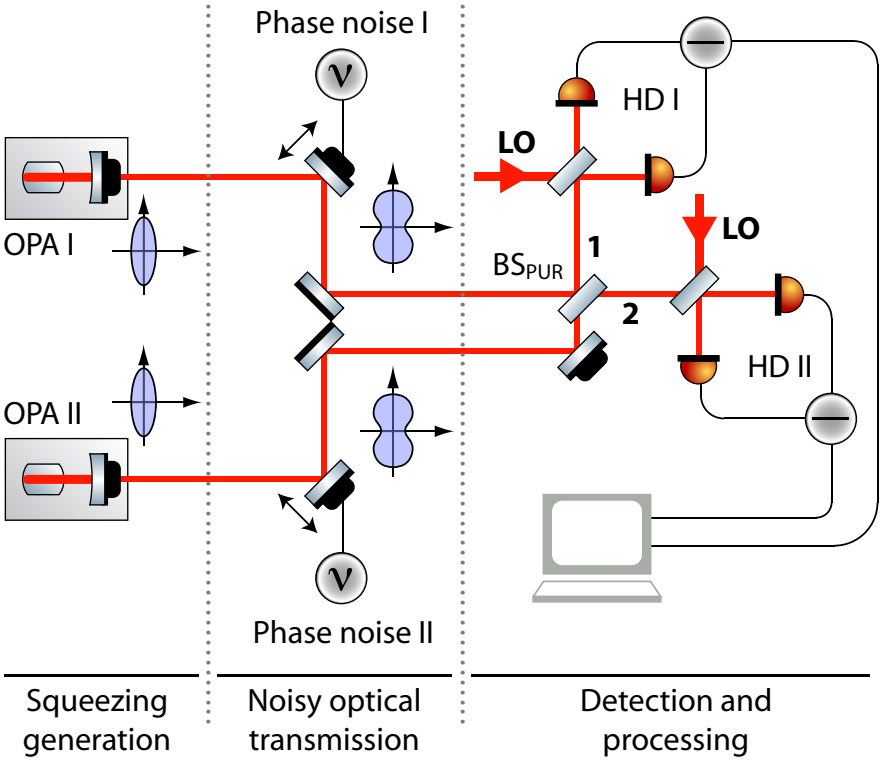

Figure 1. Schematic experimental setup for the demonstration of purification/distillation of phase-diffused squeezed states. Two optical parametric amplifiers (OPAI and OPAII) produced one amplitude-squeezed beam each. Two piezo-electric transducers drove mirrors to induce random, gaussian-weighted phase shifts to each beam to mimic the effect of a noisy optical transmission. The two phase-diffused beams were then overlapped on a balanced (50/50) beamsplitter BS$_{\mathrm{PUR}}$. Two homodyne detectors HD I and HD II in combination with a digital data acquisition system synchronously recorded time series of measured quadrature values. HD II serves the purpose of verification and can be replaced by an arbitrary experiment, which requires a squeezed input beam.

of $\Phi(\phi)$. After random phase shifts ϕ_1 and ϕ_2 the two squeezed beams interfere on a balanced beam splitter BS$_{\mathrm{PUR}}$ which forms the core of our purification/distillation setup. After interference on BS$_{\mathrm{PUR}}$, one output beam impinges on a balanced homodyne detector HD I, which measures a certain quadrature operator $q_1(\theta) = x_1 \cos\theta + p_1 \sin\theta$ of the first output mode. The purification/distillation succeeds and the state in the output mode 2 is accepted if $|q_1| < Q$. Otherwise the purification/distillation fails and the state in mode 2 is rejected. In the experiment, the purified state in mode 2 is monitored using homodyne detector HD II which allows us to determine the performance of the purification/distillation and verify its success. Our probabilistic purification and distillation scheme reduces the phase noise, enhances the squeezing and purity of the state and gaussifies it. The distinct advantage of our approach is that it relies solely on passive linear optics and balanced homodyne detection which is highly efficient and much easier to implement compared to other approaches such as projections onto vacuum state

by conditioning on no-clicks of single-photon detectors.

2.1. Experimental setup

Let us now describe our experimental setup in more detail. The sources of our squeezed states were two optical parametric amplifiers (OPAs) operated below threshold. Each device was constructed from a type I noncritically phase-matched MgO:$LiNbO_3$ crystal. The crystals were situated inside hemilithic standing-wave resonators formed by a high-reflection coated crystal surface on one end (reflectivity at 1064 nm $r^2 > 0.999$) and an externally mounted outcoupling mirror (reflectivity at 1064 nm $r^2 = 0.947$) on the other end. The intracavity surfaces of the nonlinear crystals were antireflection coated for both the fundamental wavelength (1064 nm) and the second harmonic pump field (532 nm) of the parametric process. Our laser source was a 2 W continuous wave non-planar Nd:YAG ring laser. About 1.7 W of this laser beam was frequency doubled to 532 nm. Parts of this field were injected into the OPAs through the outcoupling mirrors for pumping the nonlinear process. Both OPA cavities were kept on resonance for the 1064 nm laser radiation. For this purpose radio-frequency phase modulated control fields on the fundamental wavelength were injected into the OPA cavities through the high-reflection coated crystal surfaces. The reflected control fields were detected and provided feedback control error signals for both OPA cavity lengths as well as for both pump field phases. The amplified error signals were then fed back to piezo-electric transducers (PZTs) to precisely position the OPA cavity outcoupling mirrors and mirrors in the optical paths of the pump fields, respectively. This enabled the stably controlled production of two beams with broadband amplitude quadrature squeezing. A nonclassical noise power reduction of more than 5 dB was directly observed using homodyne detection. The squeezing spectrum was almost white over a wide range of frequencies between approximately 5 MHz and 15 MHz. Outside this band the performance of the squeezed light sources was reduced due to phase modulation signals, technical noise at lower frequencies and the limited OPA cavity linewidths at higher frequencies.

To realistically mimic the effects of noisy optical transmission channels each squeezed beam was reflected off a highreflection mirror that was randomly shifted by a PZT. Hence, random phase shifts were introduced on the beams as they would occur when transmitting the beams through optical fibers of considerable lengths. The voltages driving the PZTs were carefully produced to meet certain criteria. Although no special form of the noise is in principle required for a purification/distillation experiment we wanted to operate in a regime where the noise has well defined properties and could be easily modeled theoretically. Two independent random number generators produced data strings with a white Gaussian distribution. Both strings were then digitally filtered to limit the noise frequency band to 1–5 kHz. Performing homodyne detection on each of the beams confirmed that the amount of squeezing degraded in the same way when the strength of the phase noise was increased, see Fig. 2 (black curve/circles). Each homodyne detector was constructed from a matched pair of ETX-500 high-efficiency

photo diodes. Homodyne visibilities were at 98.4% for HD I and 98.7% for HD II.

In order to demonstrate purification/distillation the two phase-diffused squeezed beams were overlapped on a balanced (50/50) beamsplitter. Here, a visibility of 98.2% was achieved. The relative phase of the two beams on the beamsplitter was actively controlled (with a control loop bandwidth *below* the phase noise frequency band) using phase modulation sidebands present on the squeezed beams. The output beams from the beamsplitter were then detected using the homodyne detectors HD I and HD II, each of which was servo-controlled to detect the appropriate quadratures (again with feedback control loop bandwidths *smaller* than the phase noise frequencies). Each detector difference current was subsequently electronically mixed with a 7 MHz local oscillator. The demodulated signals were then filtered with steep low-pass filters (anti-aliasing filters) at 40 kHz and synchronously sampled with 100 kHz. The nonlinear phase response of these filters was digitally compensated to regain a constant group delay. Both time series of quadrature values from HD I and HD II, respectively, were then postprocessed to perform different purification/distillation protocols.

2.2. Theoretical description

In this section we derive the formula for the squeezed-quadrature variance $V_{\rm out} \equiv \langle(\Delta x_2)^2\rangle$ of the purified output state of our protocol. We consider the general scenario in which a quadrature $q_1(\theta) = x_1\cos\theta + p_1\sin\theta$ is measured by HD I and a positive purification/distillation trigger signal is provided if $|q_1| < Q$. Again, we use x_j and p_j to denote the amplitude or phase quadrature of the jth beam, respectively. We assume that before phase randomization the x quadrature of each beam is squeezed and that there are no correlations between x and p quadratures. The covariance matrix of each squeezed mode thus attains a diagonal form, $\gamma = {\rm diag}(V_x, V_p)$, where V_x and V_p denote variances of x and p quadratures. For the vacuum state we have $V_x = V_p = 1$ and the mode is squeezed if $V_x < 1$. Recall that $V_xV_p \geq 1$ as a consequence of the Heisenberg uncertainty relation.

Assume for a moment that the random phase shifts ϕ_j on each mode are fixed. Let $V_{xj} = V_x\cos^2\phi_j + V_p\sin^2\phi_j$ and $V_{pj} = V_p\cos^2\phi_j + V_x\sin^2\phi_j$, $j = 1, 2$, denote the variances of x and p quadratures of phase-shifted squeezed states impinging on $\mathrm{BS_{PUR}}$. For a fixed ϕ_j, the two-mode state at the output of $\mathrm{BS_{PUR}}$ and prior to conditioning measurement is Gaussian. Consequently, the joint probability distribution of quadratures $q_1(\theta)$ of mode 1 and x_2 of mode 2 at the output of $\mathrm{BS_{PUR}}$ is also Gaussian and reads,

$$P_{12}(q_1, x_2) = \frac{1}{2\pi\sqrt{D}}\exp\left[-\frac{Bq_1^2 + Ax_2^2 - 2Cq_1x_2}{2D}\right]. \tag{2}$$

Here $D = AB - C^2$, A and B are variances of quadratures q_1 and x_2 evaluated for the state at the output of $\mathrm{BS_{PUR}}$,

$$A = \frac{V_{x1} + V_{x2}}{2}\cos^2\theta + \frac{V_{p1} + V_{p2}}{2}\sin^2\theta$$

$$+\frac{V_p-V_x}{4}[\sin(2\phi_1)+\sin(2\phi_2)]\sin(2\theta),$$
$$B=\frac{V_{x1}+V_{x2}}{2}. \tag{3}$$

The correlation between the quadratures $C=\langle\Delta q_1\Delta x_2\rangle$ reads

$$C=\frac{V_{x1}-V_{x2}}{2}\cos\theta+\frac{V_p-V_x}{4}[\sin(2\phi_1)-\sin(2\phi_2)]\sin\theta. \tag{4}$$

The non-normalized distribution of x_2 conditional on $|q_1|<Q$ reads

$$P_{\rm cond}(x_2)=\int_{-Q}^{Q}P_{12}(q_1,x_2)dq_1. \tag{5}$$

If the phase fluctuations are symmetric, $\Phi(-\phi)=\Phi(\phi)$ then the mean value of the quadrature x_2 of the purified state is zero and we shall assume that this holds throughout the rest of the paper. The variance $V_{\rm out}$ of quadrature x_2 then becomes equal to $\langle x_2^2\rangle$ calculated from the conditional probability distribution (5), averaged over all random phase shifts and properly normalized,

$$V_{\rm out}=\frac{1}{\mathcal{P}}\int_{\phi_1}\int_{\phi_2}\int_{-\infty}^{\infty}x_2^2P_{\rm cond}(x_2)dx_2\Phi(\phi_1)\Phi(\phi_2)d\phi_1d\phi_2, \tag{6}$$

where

$$\mathcal{P}=\int_{\phi_1}\int_{\phi_2}\int_{-\infty}^{\infty}P_{\rm cond}(x_2)dx_2\Phi(\phi_1)\Phi(\phi_2)d\phi_1d\phi_2 \tag{7}$$

is the probability of successful purification/distillation. The integration over x_2 can be explicitly carried out and after some algebra we arrive at

$$V_{\rm out}=\frac{1}{\mathcal{P}}\int_{\phi_1}\int_{\phi_2}\left[B\,{\rm erf}\left(\frac{Q}{\sqrt{2A}}\right)-\sqrt{\frac{2}{\pi}}\frac{C^2Q}{A^{3/2}}e^{-\frac{Q^2}{2A}}\right]\Phi(\phi_1)\Phi(\phi_2)d\phi_1d\phi_2. \tag{8}$$

We also obtain a simplified formula for the success probability,

$$\mathcal{P}=\int_{\phi_1}\int_{\phi_2}{\rm erf}\left(\frac{Q}{\sqrt{2A}}\right)\Phi(\phi_1)\Phi(\phi_2)d\phi_1d\phi_2. \tag{9}$$

For comparison we also calculate the variance of the x quadrature of the phase-diffused state before purification/distillation,

$$V_{\rm in}=\int_{\phi}(V_x\cos^2\phi+V_p\sin^2\phi)\Phi(\phi)d\phi. \tag{10}$$

Successful purification/distillation increases the squeezing which is indicated by $V_{\rm out}<V_{\rm in}$. Note that $V_{\rm out}\geq V_x$ would always hold and the purification/distillation cannot reduce $V_{\rm out}$ below the variance V_x of the original state before transmission through a noisy channel. However, the method can restore the squeezing lost due to the phase fluctuations (or other non-Gaussian noise). After purification/distillation, the state also becomes gaussified and its purity increases [32, 33], which clearly demonstrates that our method meets all requirements imposed on a proper purification/distillation protocol.

Non-unit detection efficiency $\eta<1$ of the homodyne detectors can be easily incorporated in our theoretical model by making substitutions $V_{xj}\mapsto\eta V_{xj}+1-\eta$ and $V_{pj}\mapsto\eta V_{pj}+1-\eta$. Here we assume for the sake of simplicity that the detection efficiency

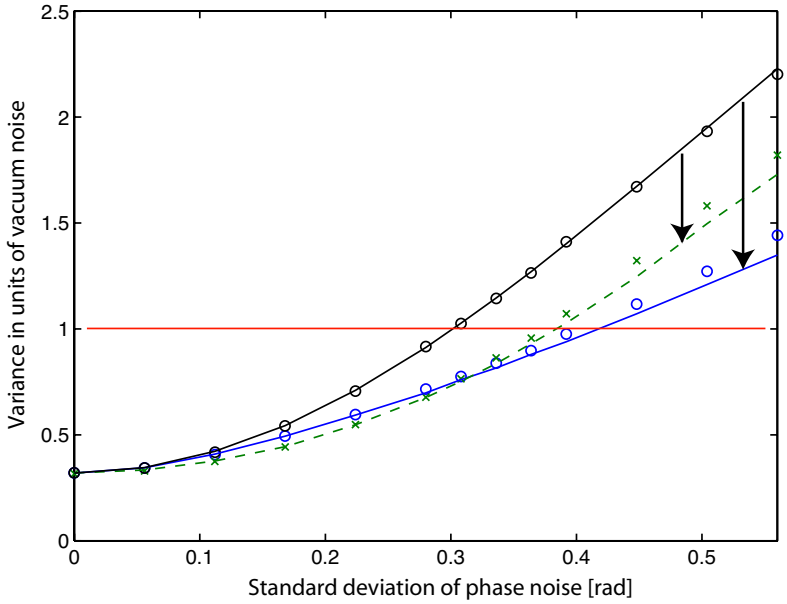

Figure 2. Demonstration of successful distillation of squeezed states for two different trigger strategies versus strength of phase fluctuations σ. Shown are measured variances of the (initially) squeezed quadrature for the phase diffused input states $V_{\rm in}$ (top, black) and for distilled states $V_{\rm out}$, when conditioned on the squeezed quadrature $|x_1| < Q$ (circles, blue) and when conditioned on the anti-squeezed quadrature $|p_1| < Q$ (crosses, green), respectively. Theoretical values are represented by solid and dashed lines. Here, the trigger threshold was set to $Q = 1.0$. For $\sigma < 0.3$ conditioning on the anti-squeezed quadrature was more efficient than conditioning on the squeezed quadrature. Red line indicates the shot-noise level. Without phase diffusion the squeezed state variances were measured to $V_x = 0.32$ and $V_p = 8.5$.

is the same for the triggering detector HD I and the verification detector HD II which monitors the purified state. If V_x and V_p are determined by homodyne detection then these measured values already include the effects of the non-unit detection efficiency and can be directly inserted into the above formulas.

2.3. Experimental results

The variances of the squeezed and anti-squeezed quadratures of the states employed in the experiment read $V_x = 0.32$ and $V_p = 8.5$ as directly measured by a homodyne detector. The states generated by the two OPAs were practically identical and the strength of the phase noise in the two channels was always kept equal. Under these circumstances, the variance $V_{\rm in}$ becomes equal to the variance of quadrature x_1 (and also x_2) at the output of $\mathrm{BS_{PUR}}$ and can be directly measured with HD I or HD II of the setup shown in Fig. 1. In Fig. 2 we compare the conditioning on measurements of the originally squeezed (x_1) and anti-squeezed (p_1) quadratures for a fixed threshold Q and varying phase noise σ. Shown are both the experimental data and the corresponding

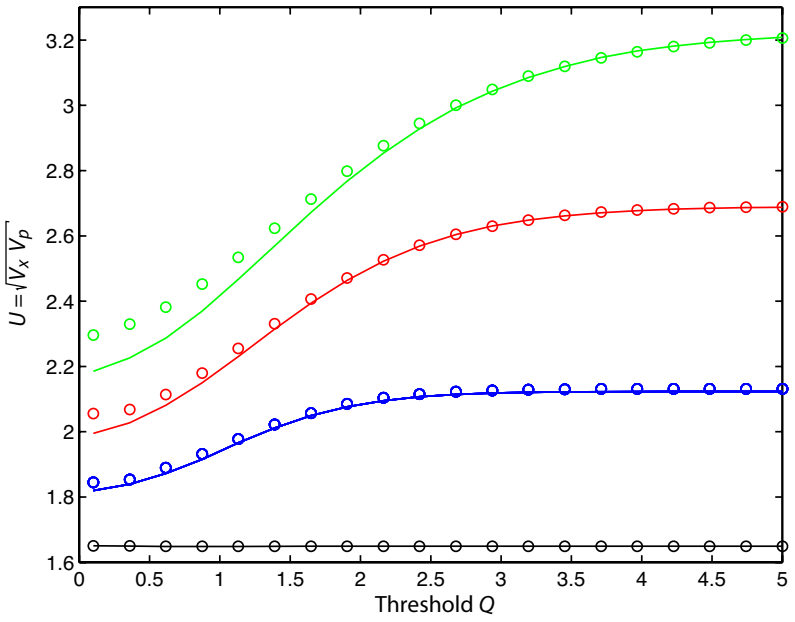

Figure 3. Uncertainty product $U = \sqrt{V_x V_p}$ of purified states for different phase noise levels ($\sigma = 0.40$ (green), $\sigma = 0.28$ (red), $\sigma = 0.17$ (blue) and $\sigma = 0$ (black)). Lines represent theoretical simulations while circles illustrate measurements.

theoretical predictions. We can clearly see that the purification/distillation enhances the squeezing and $V_{\rm out} < V_{\rm in}$. We can say that the squeezing has been probabilistically concentrated from two noisy de-phased copies of the state into a single copy which thus exhibits higher squeezing. Remarkably, the conditioning on $|p_1| < Q$ not only enhances the squeezing of the quadrature x_2 but for sufficiently weak phase noise it even leads to higher reduction of fluctuations of x_2 than conditioning on $|x_1| < Q$. This is somewhat surprising, because naively one could expect that conditioning on $|p_1| < Q$ would rather reduce the fluctuations of quadrature p_2 and enhance fluctuations of x_2. From a semiclassical point of view one could argue that small values of p_1 are detected by HD I with highest probability when the phase shifts ϕ_1 and ϕ_2 are such that the states impinging on $\mathrm{BS}_{\rm PUR}$ are both squeezed in p quadratures. However, this picture is generally oversimplified. Some insight into why conditioning on $|p_1| < Q$ can help can be gained from the expression for the output variance (8) which consists of two terms. The first term proportional to B can be interpreted as corresponding to the probing of the channel. In case of measurement of the originally squeezed quadrature x_1, the factor $\mathrm{erf}(Q/\sqrt{2A})$ is maximized for zero random phase shifts. In this case B attains its minimum value $B = V_x$, so the conditioning acts as a filter that suppresses contributions corresponding to large unwanted random phase shifts. However, formula (8) contains also second negative term, proportional to C^2Q, that always reduces the variance $V_{\rm out}$. This second distillation mechanism is of purely quantum nature since

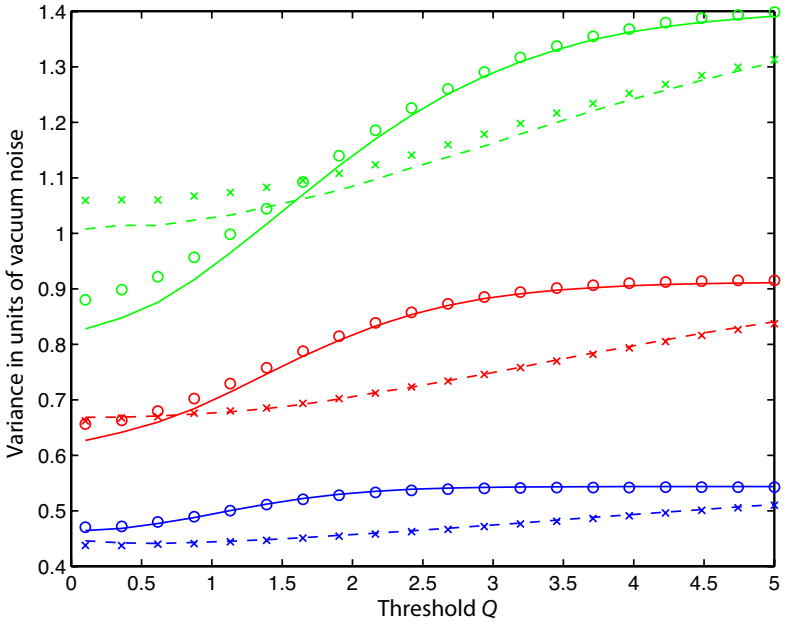

Figure 4. Quadrature variances of distilled squeezed states $V_{\rm out}$ versus trigger threshold Q. $V_{\rm out}$ is plotted for three different levels of phase noise ($\sigma = 0.40$ (green), $\sigma = 0.28$ (red) and $\sigma = 0.17$ (blue)). Results are presented for conditioning on the (initially) squeezed quadrature x_1 (solid lines, circles) and for conditioning on the antisqueezed quadrature p_1 (dashed lines, crosses). Again lines represent theoretical simulations while circles and crosses illustrate measurements.

it is a consequence of the quantum correlations established by the interference of the two copies of the de-phased state on the purifying balanced beam splitter $\mathrm{BS}_{\rm PUR}$. In case of measurements of squeezed quadrature both above mechanisms contribute to the reduction of $V_{\rm out}$. In contrast, for measurements of the anti-squeezed quadrature the first positive term increases the $V_{\rm out}$ since in this case $\mathrm{erf}(Q/\sqrt{2A})$ is maximized for phase shifts $\phi_1 = \phi_2 = \pi/2$ when B attains its maximum possible value V_p. Thus in this case the variance $V_{\rm out}$ is reduced solely due to the second negative term. Remarkably, this quantum distillation mechanism is efficient enough to reduce the fluctuations of x_2. So this conjugate purification/distillation is a purely quantum interference effect. The purification actually reduces the variances of both conjugate quadratures x_2 and p_2 as witnessed by the decrease of the uncertainty product $U = \sqrt{V_x V_p}$, see Fig. 3. The simultaneous suppression of the noise in both conjugate quadratures is a signature of the increase of purity of the state, which for Gaussian states can be evaluated as $P = 1/\sqrt{V_x V_p} = 1/U$.

In Fig. 4 we present the dependence of the variance $V_{\rm out}$ on the trigger threshold Q for three different strengths of phase fluctuations. As expected, the output variance decreases with decreasing trigger threshold. In agreement with Fig. 2 we see again that for not-too strong fluctuations the conditioning on p_1 is superior to conditioning on x_1

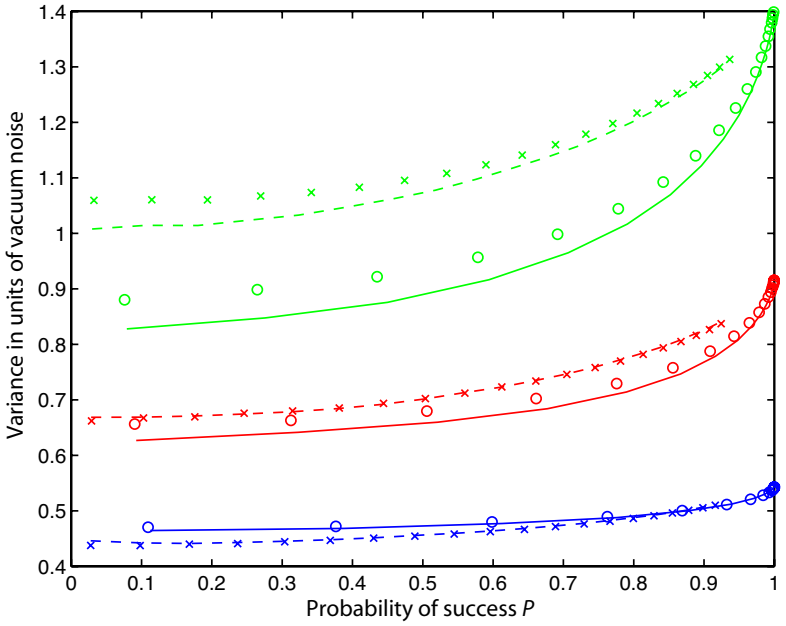

Figure 5. Illustration of the same variance data as in Fig. 4 – this time plotted over the fraction of distilled states. We refer to Fig. 4 for the detailed description of parameters used. The graphs clearly show that for weak phase noise (bottom, blue) conditioning on the antisqueezed quadrature is more efficient than conditioning on the squeezed quadrature. The opposite is found for strong phase fluctuations (top, green).

and yields lower variance $V_{\rm out}$. The probability of success $\mathcal{P}$ monotonically increases with Q but also depends on the choice of quadrature used for conditioning. For further comparison, we plot in Fig. 5 the trade-off between the output variance $V_{\rm out}$ and the success rate $\mathcal{P}$. We can see that we can achieve higher reduction of the noise at the expense of lower success rate $\mathcal{P}$. Note also that the achieved reduction of squeezed-quadrature variance is almost maximal already for $\mathcal{P}$ of the order of 30% and further lowering of the success probability results only in marginal improvement of the squeezing. This result is rather generic as confirmed by extensive numerical simulations. We can conclude that a single iteration of the purification/distillation procedure typically exhibits nearly optimum performance for a rather high success probability of several tens of percent. What is remarkable, for weak phase noise the conditioning on originally anti-squeezed quadrature p_1 yields for a given success rate $\mathcal{P}$ a lower variance $V_{\rm out}$ than conditioning on the originally squeezed quadrature x_1. For strong phase noise, however, it becomes preferential to condition on measurements of x_1. Note that the theoretical curves obtained from the simple theory developed in Sec. 2.2 are in excellent agreement with the experimental data and the theory faithfully describes all features of our purification/distillation protocol.

We have also considered conditioning on measurements of arbitrary quadrature $q_1(\theta)$ and investigated the dependence of the performance of the purification/distillation

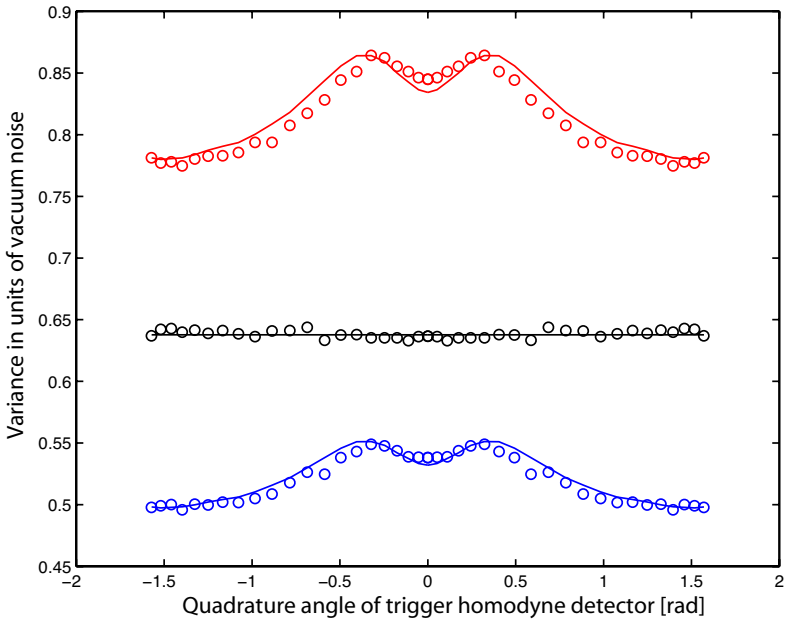

Figure 6. Experimental and theoretical characterization of our distillation protocol for phase noise $\sigma = 0.202$ and trigger threshold $Q = 0.7$. Shown are variances versus the conditioning quadrature angle. The central (black) curve shows the variance of the dephased state's amplitude quadrature $V_{\rm in}$. The lower (blue) curve shows the variance of the distilled states' amplitude quadrature $V_{\rm out}$. For this particular parameter regime conditioning on the antisqueezed quadrature works more efficiently than conditioning on the squeezed quadrature. However, the distillation protocol is successful for conditioning on *any* quadrature. The top (red) curve displays the purified variance $V_{\rm out}$ after normalizing to $V_{\rm in}$ (black curve).

protocol on θ. We have found that it in fact does not matter too much which quadrature $q_1(\theta)$ is measured in the homodyne detector HD I and the purification/distillation actually works well for all θ. Typical dependence of the squeezing of the purified state on θ is depicted in Fig. 6. We can see that $V_{\rm out}$ exhibits a local minimum at $\theta = 0$ but the global minimum corresponding to the optimal purification/distillation strategy occurs in this case at $\theta = \pi/2$. Importantly, the quadrature fluctuations are suppressed and the squeezing is thus enhanced for any θ. This implies that the purification/distillation works even with phase-randomized homodyning, where the relative phase θ between balanced homodyne detector and signal is varied or randomly fluctuates in time. Interestingly, the phase-randomized homodyning very closely resembles the vacuum projection considered in Refs. [26, 27]. The effective Positive Operator Valued Measure (POVM) element that describes this conditioning measurement reads

$$\Pi_Q = \frac{1}{2\pi}\int_0^{2\pi}\int_{-Q}^{Q} |q;\theta\rangle\langle q;\theta|\, d\theta\, dq = \sum_{n=0}^{\infty} P_n |n\rangle\langle n|, \tag{11}$$

where $|q;\theta\rangle$ is the eigenstate of operator $q_1(\theta)$ with eigenvalue q and P_n =

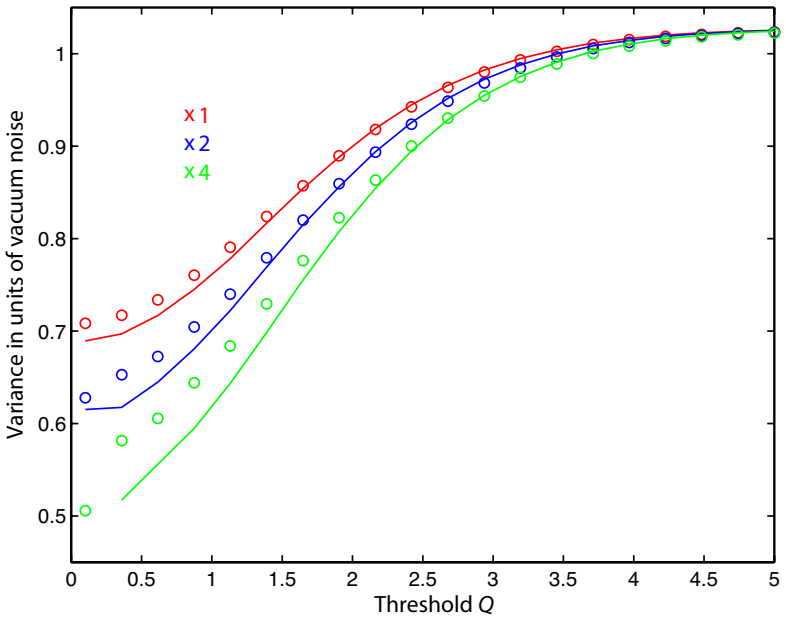

Figure 7. The effect of quantum channel probing is shown by plotting the variance of the purified state $V_{\rm out}$ over the chosen threshold. The red curve corresponds to the previously described method. The blue and green curves result, when conditioning is commenced on two and four subsequent values, respectively.

$(\sqrt{\pi}2^n n!)^{-1} \int_{-Q}^{Q} H_n^2(x) e^{-x^2} dx$, where $H_n(x)$ denotes the Hermite polynomial. Π_Q is diagonal in the Fock state basis because all off-diagonal terms vanish due to averaging over random phase shift θ. The dominant part of this POVM element is the term proportional to the projector onto vacuum state $|0\rangle$, but Π_Q also contains terms proportional to projectors onto higher Fock states $|n\rangle$. This POVM can be thus considered as an approximate noisy version of the ideal projection onto vacuum.

3. Enhancement by Quantum Channel Probing

In the previous sections we have analyzed several strategies for conditioning in our two-copy purification and distillation protocol. In this section we investigate a classical enhancement for our protocol. Since a lot of copies of the decohered quantum state are sent through the same channel they might be used as quantum probes providing information about the channel. This approach can be used to classically improve our purification/distillation protocol if the phase noise (or at least parts of it) occurs at frequencies well below the resolution bandwidth with which optical states are measured. In this case the random phase shifts of subsequently arriving copies of squeezed states are not completely independent. Here, we propose a protocol which exploits these correlations between phase fluctuations of several subsequent copies of the state which we term *quantum channel probing* (*QCP*). Since QCP is an extension of the post-

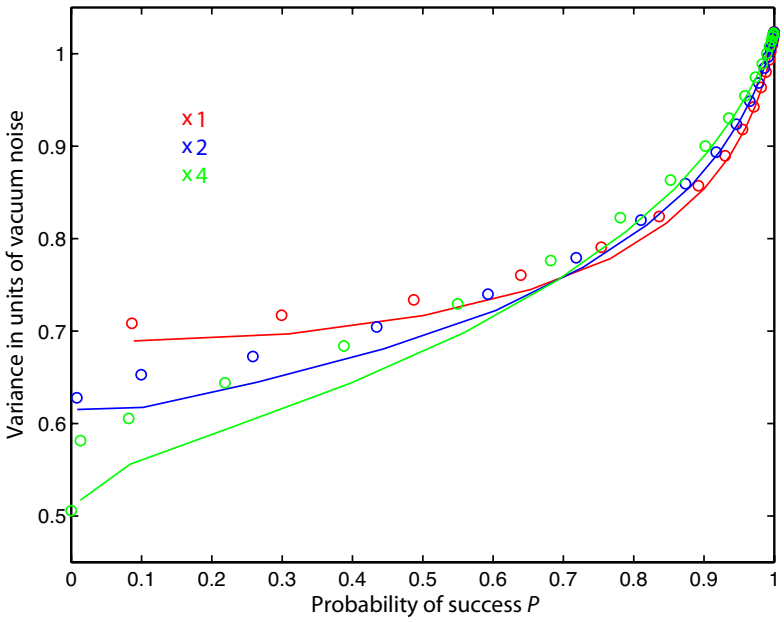

Figure 8. The same data as in figure 7 is displayed, this time plotted over the probability of success. It should be noted that applying the method of *quantum channel probing* does not necessarily improve the squeezed quadrature's variance when a given rate of survivors is to be achieved. For a probability of success smaller than approximately 0.75, though, quantum channel probing yields a significant improvement.

processing stage of our purification/distillation protocol it can be (and in the following is) applied to the same data as the latter.

In QCP a positive trigger signal is generated at the homodyne detector HD I if not only a single but a certain number N_{QCP} of subsequent measurements all fulfill a certain condition $|q_1| < Q$. Since we consider the QCP as an enhancement of our purification/distillation protocol, the measurement setup still corresponds to Fig. 1 and HD I measures the quadrature $q_1(\theta) = x_1 \cos\theta + p_1 \sin\theta$. The theory presented in Sec. 2.2 can be easily generalized to describe the QCP protocol. In particular, in the limit of perfectly correlated identical random phase shifts on N_{QCP} subsequent copies we obtain the following expression for the output variance,

$$V_{\mathrm{out}} = \frac{1}{\mathcal{P}_{\mathrm{QCP}}} \int_{\phi_1}\int_{\phi_2} \left[B \,\mathrm{erf}\left(\frac{Q}{\sqrt{2A}}\right) - \sqrt{\frac{2}{\pi}}\frac{C^2 Q}{A^{3/2}} e^{-\frac{Q^2}{2A}} \right] \times \left[\mathrm{erf}\left(\frac{Q}{\sqrt{2A}}\right)\right]^{N_{\mathrm{QCP}}-1} \Phi(\phi_1)\Phi(\phi_2) d\phi_1 d\phi_2. \tag{12}$$

Here

$$\mathcal{P}_{\mathrm{QCP}} = \int_{\phi_1}\int_{\phi_2} \left[\mathrm{erf}\left(\frac{Q}{\sqrt{2A}}\right)\right]^{N_{\mathrm{QCP}}} \Phi(\phi_1)\Phi(\phi_2) d\phi_1 d\phi_2. \tag{13}$$

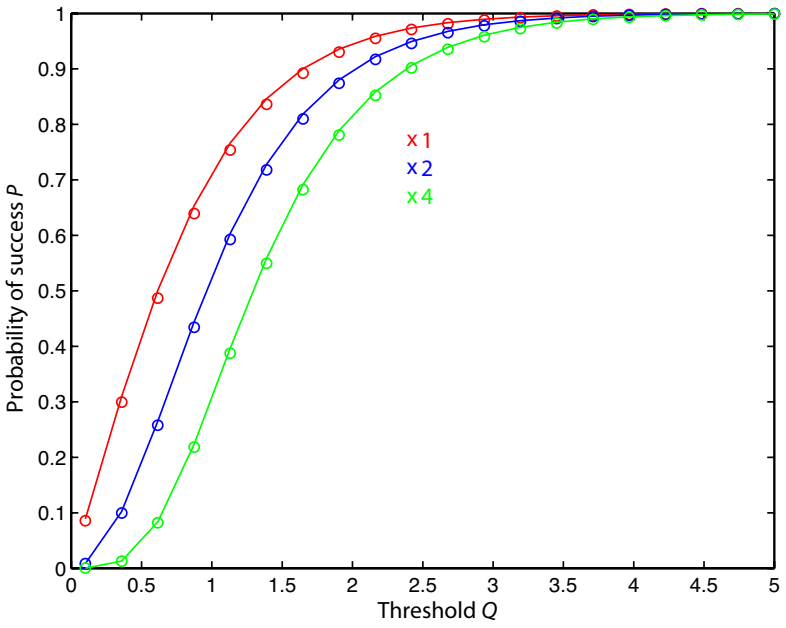

Figure 9. This figure shows the interdependence between the chosen threshold Q and the rate of survivors when the method of quantum channel probing is applied. As before, the red, blue and green curves correspond to one, two and four subsequent triggers (lines: theoretical predictions, circles: measured values).

is the probability of success of the QCP protocol. The effect of QCP is represented by additional factors $[\mathrm{erf}(Q/\sqrt{2A})]^{N_{\mathrm{QCP}}-1}$ in Eqs. (12) and (13) compared to Eqs. (8) and (9).

If the observed quadrature $q_1(\theta)$ is the initially squeezed one $q_1(0) = x_1$ this protocol probes the alignment of the squeezing ellipses of the input states because the condition $|q_1| < Q$ for more than one subsequent measurement is more likely met if the lean axes of the squeezing ellipses match the quadrature of the homodyne detector, i.e. the zero-crossing of the phase fluctuations. The results are shown in Fig. 7, Fig. 8 and Fig. 9. In all cases the QCP enhanced distillation protocol was conditioned on the initially squeezed amplitude quadrature. Fig. 7 shows the enhancement for $N_{\mathrm{QCP}} = 2$ (blue) and $N_{\mathrm{QCP}} = 4$ (green) subsequent triggers in comparison with $N_{\mathrm{QCP}} = 1$, which corresponds to the original setup. From Fig. 9 one can see that for a given threshold Q the probability of success drops quite a bit with increasing N_{QCP} but Fig. 8 shows that the improvement in the variance overcomes the decrease of success probability.

We emphasize that no improvement was found when the trigger was generated from a measurement of the anti-squeezed quadrature. Fig. 10 shows that in this case the distillation protocol was in fact even less efficient. This is not surprising because in this latter case the QCP acts against the conjugate purification mechanism represented by the negative term in Eq. (12), c.f. also discussion in Sec. 2.3.

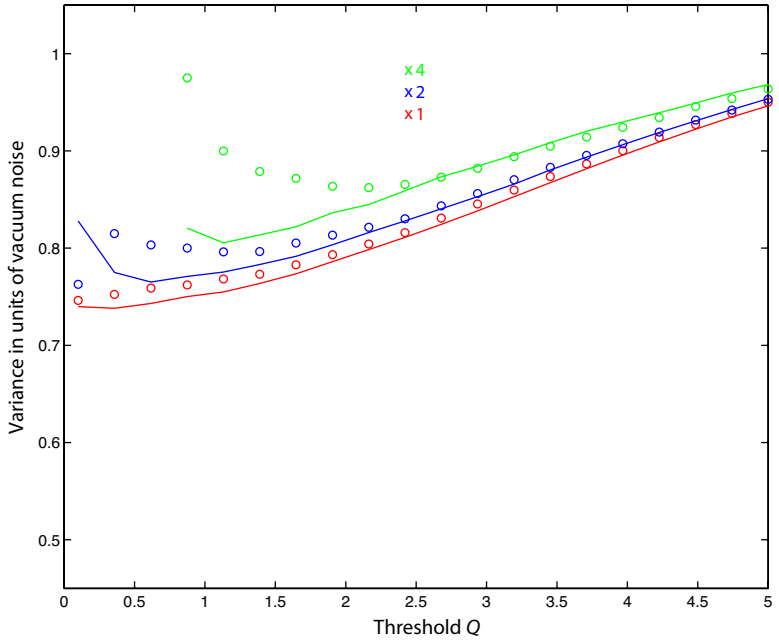

Figure 10. The QCP does not work when the trigger homodyne detector HD I is tuned to measure p_1. Thus it is more obvious that our protocol is more than just classical channel probing. As before, the red, blue and green curves correspond to one, two and four subsequent triggers (lines: theoretical predictions, circles: measured values).

4. Conclusions

We performed and analyzed an experiment that demonstrated several strategies for conditioning the purification/distillation of phase-diffused squeezed states. Two copies of the decohered states were overlapped on a beam splitter and one beam splitter output was detected with a balanced homodyne detector to provide a trigger signal. In case of such a trigger event, states with regained squeezing strength were found at the second beam splitter output. In all cases we also found that the distilled states had a higher *purity*. Detection of the second beam is not required for the protocol and the purified state is thus available for further applications. This should be contrasted with purification of polarization-entangled states of two photons, where the determination of the success of the purification procedure requires destructive detection of the purified photons [36]. Our theoretical and experimental results show that good trigger signals could be generated from arbitrary quadratures including the originally anti-squeezed one. This is possible due to the quantum interference of the two copies of the phase-diffused state on the purifying beam splitter which creates quantum correlations between the quadratures of the two output beams. This result is also of practical relevance. It means that the local oscillator of the homodyne detector that produces the trigger

signal does not need to be phase locked. Hence one control loop can be saved. The experimental result was in excellent agreement with our theoretical predictions. Very good to excellent agreement between experiment and theory was also found for the observed quality of our purification/distillation protocol in dependence on the phase noise strength, the trigger threshold value and the number of purified states with respect to the number of input states.

We also proposed to enhance our purification/distillation protocol by quantum channel probing. This add-on utilizes classical correlations between decohered states transmitted through the same channel. With this extension the purification/distillation protocol could further be optimized, however, the trigger quadrature had to be the squeezed quadrature. Triggering on the anti-squeezed quadrature failed in this case. This observation clearly draws a line between a purification/distillation protocol that builds on quantum correlations between two copies, and a quantum channel probing protocol that builds on classical correlations between states subsequently transmitted through the channel.

Acknowledgments

We acknowledge financial support from the Deutsche Forschungsgemeinschaft (DFG), project number SCHN 757/2-1. J.F. acknowledges financial support from the Ministry of Education of the Czech Republic under the projects Centre for Modern Optics (LC06007) and Measurement and Information in Optics (MSM6198959213) and from the EU under project COVAQIAL (FP6-511004). P.M. acknowledges financial support from the European Social Fund. Furthermore we thank R. Filip for stimulating discussions.

References

[1] S. L. Braunstein and P. van Loock, Rev. Mod. Phys. **77**, 513 (2005).
[2] Z. Y. Ou, S. F. Pereira, H. J. Kimble and K. C. Peng, Phys. Rev. Lett. **68**, 3663 (1992).
[3] R. Schnabel, W. P. Bowen, N. Treps, H.-A. Bachor, T. C. Ralph und P. K. Lam, Phys. Rev. A **67**, 012316 (2003).
[4] F. Grosshans, G. Van Assche, J. Wenger, R. Brouri, N. J. Cerf, and Ph. Grangier, Nature (London) **421**, 238 (2003).
[5] A. Furusawa, J. L. Sørensen, S. L. Braunstein, C. A. Fuchs, H. J. Kimble and E. S. Polzik, Science **282**, 706 (1998).
[6] W. P. Bowen, N. Treps, B. C. Buchler, R. Schnabel, T. C. Ralph, H.-A. Bachor, T. Symul, and P.-K. Lam, Phys. Rev. A **67**, 032302 (2003).
[7] B. Julsgaard, A. Kozhekin, and E.S. Polzik, Nature (London) **413**, 400 (2001).
[8] B. Julsgaard, J. Sherson, J. I. Cirac, J. Fiurášek, and E. S. Polzik, Nature (London) **432**, 482 (2004).
[9] J.F. Sherson, H. Krauter, R.K. Olsson, B. Julsgaard, K. Hammerer, I. Cirac, and E. S. Polzik, Nature (London) **443**, 557 (2006).
[10] Ch. Silberhorn, P. K. Lam, O. Weiss, F. König, N. Korolkova, and G. Leuchs, Phys. Rev. Lett. **86**, 4267 (2001).
[11] C. Schori, J. L. Sorensen, and E.S. Polzik, Phys. Rev. A **66**, 033802 (2002).
[12] W. P. Bowen, N. Treps, R. Schnabel, and P.-K. Lam, Phys. Rev. Lett. **89**, 253601 (2002).

[13] W. P. Bowen, R. Schnabel, P. K. Lam und T. C. Ralph, Phys. Rev. Lett. **90**, 043601 (2003).
[14] W. P. Bowen, N. Treps, B. C. Buchler, R. Schnabel, T. Symul, T. C. Ralph und P. K. Lam, IEEE J SEL TOP QUANT, **9** (6), 1519 (2003).
[15] J. Jing, J. Zhang, Y. Yan, F. Zhao, C. Xie, and K. Peng, Phys. Rev. Lett. **90**, 167903 (2003); J. Mizuno, K. Wakui, A. Furusawa, and M. Sasaki, Phys. Rev. A **71**, 012304 (2005).
[16] N. Takei, H. Yonezawa, T. Aoki, and A. Furusawa, Phys. Rev. Lett. **94**, 220502 (2005).
[17] U. L. Andersen, V. Josse, and G. Leuchs, Phys. Rev. Lett. **94**, 240503 (2005).
[18] G. Giedke and J. I. Cirac, Phys. Rev. A **66**, 032316 (2002).
[19] J. Eisert, S. Scheel, and M. B. Plenio, Phys. Rev. Lett. **89**, 137903 (2002).
[20] J. Fiurášek, Phys. Rev. Lett. **89**, 137904 (2002).
[21] C. H. Bennett, G. Brassard, S. Popescu, B. Schumacher, J. A. Smolin, and W. K. Wootters, Phys. Rev. Lett. **76**, 722 (1996).
[22] D. Deutsch, A. Ekert, R. Jozsa, C. Macchiavello, S. Popescu, and A. Sanpera, Phys. Rev. Lett. **77**, 2818 (1996).
[23] B. Kraus, K. Hammerer, G. Giedke, and J. I. Cirac, Phys. Rev. A **67**, 042314 (2003).
[24] L.-M. Duan, G. Giedke, J. I. Cirac, and P. Zoller, Phys. Rev. Lett. **84**, 4002 (2000).
[25] T. Opatrný, G. Kurizki, and D.-G. Welsch, Phys. Rev. A **61**, 032302 (2000).
[26] D. E. Browne, J. Eisert, S. Scheel, and M. B. Plenio, Phys. Rev. A **67**, 062320 (2003).
[27] J. Eisert, D. E. Browne, S. Scheel, and M. B. Plenio, Ann. Phys. **311**, 431 (2004).
[28] A. Ourjoumtsev, R. Tualle-Brouri, J. Laurat, and Ph. Grangier, Science **312**, 83 (2006).
[29] J. S. Neergaard-Nielsen, B. Melholt Nielsen, C. Hettich, K. Mølmer, and E. S. Polzik, Phys. Rev. Lett. **97**, 083604 (2006).
[30] A. Ourjoumtsev, A. Dantan, R. Tualle-Brouri, and Ph. Grangier, quant-ph/0608230.
[31] K. Wakui, H. Takahashi, A. Furusawa, M. Sasaki, quant-ph/0609153.
[32] J. Fiurášek, P. Marek, R. Filip, and R. Schnabel, Phys. Rev. A **75**, 050302(R) (2007).
[33] A. Franzen, B. Hage, J. DiGuglielmo, J. Fiurášek, and R. Schnabel, Phys. Rev. Lett. **97**, 150505 (2006).
[34] J. Heersink, Ch. Marquardt, R. Dong, R. Filip, S. Lorenz, G. Leuchs, and U. L. Andersen, Phys. Rev. Lett. **96**, 253601 (2006).
[35] O. Glöckl, U. L. Andersen, R. Filip, W. P. Bowen, and G. Leuchs, Phys. Rev. Lett. **97**, 053601 (2006).
[36] J.-W. Pan, S. Gasparoni, R. Ursin, G. Weihs, and A. Zeilinger, Nature **423**, 417 (2003).